Paleoceanography and Paleoclimatology

RESEARCH ARTICLE
10.1029/2022PA004546

Key Points:

- Coral skeletal phosphorus content with scattered nitrogen isotopes is reconstructed over the past 400 years
- Nutrient supply declined up to 48% since the Little Ice Age in the western South China Sea
- The coral record from links nutrient supply to monsoon wind, implying higher productivity under a stronger monsoon in the future

Supporting Information:

Supporting Information may be found in the online version of this article.

Correspondence to:

M. Chen and P. Martin,
mengli.chen@nus.edu.sg;
pmartin@ntu.edu.sg

Citation:

Chen, M., Martin, P., Ren, H., Zhang, R., Samanta, D., Chen, Y.-C., et al. (2023). Enhanced monsoon-driven upwelling in Southeast Asia during the Little Ice Age. *Paleoceanography and Paleoclimatology*, *38*, e2022PA004546. https://doi.org/10.1029/2022PA004546

Received 14 SEP 2022
Accepted 1 APR 2023

Author Contributions:

Conceptualization: Mengli Chen, Patrick Martin, Konrad A. Hughen, Nathalie F. Goodkin
Data curation: Konrad A. Hughen
Formal analysis: Dhrubajyoti Samanta
Funding acquisition: Haojia Ren, Nathalie F. Goodkin
Investigation: Mengli Chen, Patrick Martin, Haojia Ren, Yi-Chi Chen
Methodology: Mengli Chen, Patrick Martin, Haojia Ren, Run Zhang, Dhrubajyoti Samanta, Yi-Chi Chen, Konrad A. Hughen, Kim Hoang Phan, Si Tuan Vo, Nathalie F. Goodkin
Project Administration: Konrad A. Hughen, Kim Hoang Phan, Si Tuan Vo, Nathalie F. Goodkin
Resources: Haojia Ren, Run Zhang, Kim Hoang Phan, Nathalie F. Goodkin
Software: Dhrubajyoti Samanta
Supervision: Nathalie F. Goodkin

Enhanced Monsoon-Driven Upwelling in Southeast Asia During the Little Ice Age

Mengli Chen[1,2], Patrick Martin[3], Haojia Ren[4], Run Zhang[5], Dhrubajyoti Samanta[1,3], Yi-Chi Chen[4], Konrad A. Hughen[6], Kim Hoang Phan[7], Si Tuan Vo[7], and Nathalie F. Goodkin[1,3,8]

[1]Earth Observatory of Singapore, Nanyang Technological University, Singapore, Singapore, [2]Tropical Marine Science Institute, National University of Singapore, Singapore, Singapore, [3]Asian School of the Environment, Nanyang Technological University, Singapore, Singapore, [4]Department of Geosciences, National Taiwan University, Taipei, Taiwan, [5]College of Ocean and Earth Sciences, Xiamen University, Xiamen, China, [6]Department of Marine Chemistry and Geochemistry, Woods Hole Oceanographic Institution, Falmouth, MA, USA, [7]Nha Trang Institute of Oceanography, Vietnam Academy of Science and Technology, Hanoi, Vietnam, [8]Department of Earth and Planetary Sciences, American Museum of Natural History, New York, NY, USA

Abstract Climate change impacts ocean nutrient availability and will likely alter the marine food web. While climate models predict decreased average ocean productivity, the extent of these changes, especially in the marginal seas upon which large human populations depend, is not well understood. Here, we reconstructed changes in seawater phosphate concentration and nitrate source over the past 400 years, which reveals a more than 50% decline in residence time of seawater phosphate, and 8%–48% decline in subsurface nitrogen supply following the coldest period of Little Ice Age. Our data indicates a link between surface ocean nutrient supply and the East Asian Summer Monsoon strength in an economically important marginal sea. As climate models predict that the East Asian Summer monsoon will strengthen in the future, our study implies that surface ocean primary productivity may increase in the South China Sea, contrary to the predicted decrease in global average ocean productivity.

Plain Language Summary Global climate models predict that surface ocean nutrient concentrations will significantly decrease over the next 100 years as our climate changes. However, in the world's marginal seas, which human populations depend on most heavily for food security, the surface ocean biogeochemical changes are still difficult to predict with global-scale models. Here, using coral-based paleoclimate proxies, we reconstruct changes to surface phosphate concentration and to sources of surface nitrogen over the past four centuries in the South China Sea (SCS). Combined with box model simulations, our data reveal a more than 50% decline in phosphate residence time and an 8%–48% decline in subsurface nitrate supply from the 1600s to present. Such a decline implies a significant decrease in primary productivity and likely a community shift toward nitrogen-fixing phytoplankton. Importantly, our data indicate that the decrease in nutrient supply was driven by weakened monsoon-induced upwelling, demonstrating strong ties between nutrient supply and monsoon strength in the SCS. Climate change is predicted to strengthen the East Asian Summer Monsoon, and our results suggest that primary productivity in this economically important region may increase, contrary to the widely predicted decreases in average global ocean productivity.

1. Introduction

Anthropogenic climate change is predicted to stratify the world's ocean, trapping nutrients at depth, and suppressing primary productivity in the future (Fu et al., 2016; Moore et al., 2018; Pachauri et al., 2014). However, wind-driven upwelling may also act as a counter-mechanism to lessen the stratification in specific areas (Sallée et al., 2013). In areas like marginal seas and coastal regions, upon which 1.3 billion people depend for food and livelihoods (Sale et al., 2014), the extent of the biogeochemical responses to climate change is still difficult to predict with global-scale models (Boyd et al., 2014). Paleoceanographic proxy records that span periods of well-characterized climatic variability can expand our knowledge of how ocean biogeochemistry responds to changing climate. The most extensively documented period of natural and rapid climate change in the northern hemisphere is the Little Ice Age (LIA) (Mann, 2002; Moberg et al., 2005), which resulted in considerable changes to the East Asian Summer and Winter monsoon, causing both extensive floods and droughts (Buckley

Validation: Mengli Chen
Visualization: Mengli Chen, Dhrubajyoti Samanta
Writing – original draft: Mengli Chen
Writing – review & editing: Patrick Martin, Haojia Ren, Run Zhang, Dhrubajyoti Samanta, Konrad A. Hughen, Nathalie F. Goodkin

et al., 2007). In Asia, the LIA also coincided with the collapse of the Angkor Kingdom and the Ming Dynasty (Zheng et al., 2014).

Coral-based ocean biogeochemical proxy records show that the North Pacific Subtropical Gyre has expanded since the LIA, resulting in increased nitrogen fixation rates (Sherwood et al., 2014) and large changes in phytoplankton community composition (McMahon et al., 2015). Another record based on crustose coralline algae on the Labrador shelf shows reduced nitrate supply since the end of the LIA, linked to climate-driven changes in ocean circulation (Doherty et al., 2021). Although both sites reveal decreased nutrients since the LIA, the different mechanisms causing these changes underscore the fact that climatic controls over ocean biogeochemistry vary spatially (Boyd et al., 2014), and for regional oceans our understanding of ocean biogeochemical responses to climatic changes remains poor.

Massive corals that span over multiple centuries provide invaluable archives for past ocean environments. Within coral skeletons, the phosphorus to calcium ratio (P/Ca_{coral}) and the nitrogen isotope ratio ($\delta^{15}N_{coral}$) are emerging proxies that allow for reconstruction of surface ocean nutrient conditions over the multi-century life span of a colony. Here, we use a 400-year-long *Porites lutea* coral core collected from the upper 10 m in the South China Sea (SCS) near Vietnam to investigate how the nutrient biogeochemistry of one of the world's major marginal seas have been impacted by the climate changes of the LIA.

The SCS is surrounded by densely populated coastal cities dependent on it for daily subsistence (Stobutzki et al., 2006). Biogeochemical changes in the SCS, therefore, have the potential to impact the protein supply for a significant proportion of the world's population. Largely oligotrophic, the SCS has two main regions of monsoon-driven coastal upwelling, leading to a seasonal supply of nutrient-rich sub-surface waters off the coasts of Vietnam (Xie et al., 2003) and Luzon Island (northern Philippines, Figure 1; Figure S1 in Supporting Information S1). During the Winter Monsoon (November–March), nutrient-depleted water is advected from the open SCS to coastal Vietnam; while during the Summer Monsoon (June–September), the wind direction and topography generate coastal upwelling off southern Vietnam (Xie et al., 2003), bringing nutrient-rich water to the surface at and around our coral site (Loick et al., 2007) (Figure 1; Figure S1 in Supporting Information S1). The summer upwelling off the Vietnam coast has been found to impact regional climate (Xie et al., 2003) as well as biogeochemistry (Loick et al., 2007) and productivity (Loick-Wilde et al., 2017).

The P/Ca in corals has been shown to be a robust proxy for surface ocean phosphate concentration in a wide range of environments (M. Chen et al., 2019; Dodge et al., 1984; Jiang et al., 2020; LaVigne et al., 2008); with moderate variation across colonies (M. Chen et al., 2019; Dodge et al., 1984; Jiang et al., 2020; LaVigne et al., 2008; LaVigne et al., 2010; Mallela et al., 2013), and also been successfully reconstructed the surface ocean phosphate over decadal-to-centennial timescales (M. Chen et al., 2022; Mallela et al., 2013). The coral P/Ca should therefore track monsoon-induced upwelling variations in the western SCS. To complement the coral P/Ca reconstruction, the source of nitrogen (N), another macronutrient in the surface ocean, can be simultaneously tracked in the nitrogen isotopes in the coral core ($\delta^{15}N_{coral}$) (Ren et al., 2017; Wang et al., 2016). The possible sources of N to our coral site are N fixation, riverine N input, and sub-surface nitrate supplied predominantly through monsoon-driven upwelling. Of the three possible sources, the riverine N input is expected to be minor: the plumes of the two local streams, Tac and Cai, move along the shore within the bay (Nguyen et al., 2000) and remain well removed from our coral site (Bolton et al., 2014). Nutrients from the only large river in southern Vietnam, the Mekong (Figure 1), are typically consumed by primary production at least 300 km before reaching our site (Grosse et al., 2010; Loick et al., 2007), leaving nitrogen fixation and upwelling of subsurface nitrate as the only major sources of N.

Here, we measured annually resolved P/Ca to assess changes in the upwelling supply of P in this region. Additionally, we analyzed the $\delta^{15}N_{coral}$ over five time periods from the LIA to the present (1600–1610, 1710–1720, 1850–1860, 1900–1920, 1991–2000) to investigate changes in nitrogen supply during and after the LIA. Bi-monthly sampling of the coral for the years 1634, 1969, and 1994 was further used to confirm the assumed seasonality of the nutrient supply due to upwelling.

2. Materials and Methods

2.1. Coral Collection and Chronology

The coral core in this study was collected in March 2011, near the northern tip of Hôn Tré Island (12°12′49.90″N, 109°18′17.51″E). The living coral was sampled using an underwater hydraulic drill, producing a 4.6 m core,

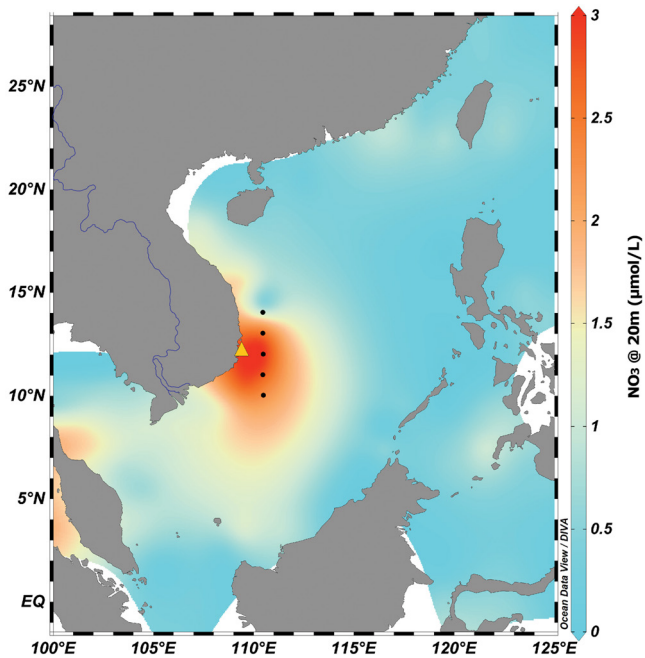

Figure 1. Map of the South China Sea showing the coral collection site (yellow triangle) and the five seawater profile sampling stations where we measured seawater nutrient and $\delta^{15}N$ (black dots) off Vietnam. The multi-year average (1955–2012) summer nitrate concentration at 20 m (which is the average mixed layer depth of the upwelling region during the upwelling season) is shown in the background color (Garcia et al., 2013). The nearest large river, the Mekong, is shown by the dark blue line.

spanning from ~1560s to 2011. The core was slabbed; cleaned several times with MilliQ water in an ultra-sonic bath; dried in an oven at 60°C, and X-rayed to reveal the annual bands and main growth axis. After drying, for quality assurance, the coral was carefully sampled over the period 1600–2004 for reconstruction. The last ~40 years from the bottom of the core was not used for reconstruction to conservatively avoid periods that had evidence of diagenesis (Goodkin et al., 2021) and potentially exchanges with the bottom substrate that alters chemical proxies. The top 5 years was also not used for reconstruction to avoid potential complication with the issue layer, which is also a conservative selection given the shallow depth of the tissue layer's influence for P/Ca in corals (LaVigne et al., 2008). After removing the top and bottom periods, the remaining ~4.2 m-long coral core contains well-preserved aragonite that is free from contact with bottom substrate or overlying seawater and is also free of diagenesis (Bolton et al., 2014; Goodkin et al., 2021).

Annual samples for P/Ca measurements were taken from aliquots of the previously sampled, age-modeled coral (Goodkin et al., 2019). The age model was developed using X-ray images, with alternating bright and dark bands corresponded to ~1 year. Potential uncertainty about the age model has been discussed in the previous study (Goodkin et al., 2019), which mainly arise from years of no/little growth for which the band is not observable. These errors are believed minimal at modern time (±1 year) but may accumulate toward the beginning of the record (±10 years) (Goodkin et al., 2019). Using the same age model, ~50–70 mg of coral powders was drilled along the main growth axis at bi-annual resolution for $\delta^{15}N$ measurement. The $\delta^{15}N$ was sampled in specific window periods in an opportunistic manner based on high and low coral P/Ca.

In addition, bi-monthly resolution samples were included in the study to illustrate the seasonal variability, including year 1634, 1969, and 1994. Samples from year 1969 were taken from aliquots from the previously drilled and age-modeled samples (Bolton et al., 2014; Goodkin et al., 2021), where the age model was developed by comparing the measured Sr/Ca in the sample with the climatological mean monthly sea surface temperature (SST). Whereas samples from year 1634 and 1994 were newly drilled at approximately 1.5 mm increments (5–7 samples/yr) along the major growth axis, with the starting and ending time aligned with the x-ray-based age model from the previous study (Goodkin et al., 2019). The newly-drilled samples were split into three aliquots, including ~200 µg for P/Ca, ~50–70 mg for $\delta^{15}N$, and ~400 µg for Sr/Ca that helps to develop the seasonal age model of the newly-drilled samples. The analysis of Sr/Ca and the age modeling have been described in detail in Bolton et al. (2014), which briefly corresponds to aligning the measured Sr/Ca in the samples with the SST climatology (Figure S2 in Supporting Information S1).

2.2. Coral P/Ca Measurement

The P/Ca in the coral was measured by a triple quadrupole Inductively Coupled Plasma Mass Spectrometer (ICP-QQQ) following the methods laid out in (M. Chen et al., 2019). Briefly, ~200 µg of the drilled coral powder was dissolved in 0.2 M nitric acid (Optima grade) and measured using a mass shift method. This method effectively removes interferences from $^{15}N^{16}O^{+}$ and $^{14}N^{16}OH^{+}$ that conventionally present a major interference for P at mass/charge = 31, and reduces the detection limit for P to about 2.0 nmol/L. The matrix effect by calcium ion was corrected by running matrix-matched standards. All plasticware was cleaned extensively by acid and yielded procedural blanks below the detection limit. The precision of the method was estimated by repeated measurement of the certified coral standard JCp-1, dissolved in a 30 mL bottle. The measured P/Ca in JCp-1 was 14.92 ± 0.55 mmol/mol ($n = 29$), within the range of the certified value of 13.2 ± 2.9 µmol/mol. We additionally analyzed 34 independently dissolved JCp-1 to illustrate the internal heterogeneity, for which we report the P/Ca as 15.17 ± 1.64 µmol/mol. The ±1.64 µmol/mol represents the total uncertainty of the analytical method after counting the heterogeneity, and compares well with the previously suggested ±1.4 µmol/mol of the skeletal heterogeneity derived from parallel drilling tracks (M. Chen et al., 2019).

2.3. Coral Skeletal $\delta^{15}N$ Measurement

The coral skeletal $\delta^{15}N$ was measured in cleaned skeleton samples by Isotope Ratio Mass Spectrometry (IRMS) through dissolution, oxidation, and the denitrifier method adopted from (Ren et al., 2017; Wang et al., 2015). Briefly, 50–70 mg of coral powder were soaked in 10 mL of sodium hypochlorite solution (10%–15% available chlorine, agitated every hour) to remove organic contaminants on the coral surface. The cleaned coral powders were rinsed 3 times in MilliQ water; dried in a vacuum oven at 60°C, and then carefully split into ∼10 mg samples in 4 mL borosilicate glass vials (Wheaton®, muffled at 500°C for 6 hr). The cleaned coral was then dissolved in 80 μL of 4M ultrapure HCl. For oxidation, 1 mL of a solution of recrystallized alkaline potassium persulfate (2% persulfate—1% NaOH) was added and autoclaved for 30 min at 121°C with a slow vent setting to oxidize all organic nitrogen into nitrate. Six procedural blanks were included in each batch of oxidation. The blank nitrate concentration averaged 0.3 ± 0.1 μM, which was typically less than 2% of the total N in each sample. The $\delta^{15}N$ of the reagent blanks was constrained by regressing the measured $\delta^{15}N$ with respect to the blank-to-total N ratio using three sets of standards at different concentrations: USGS 40 ($\delta^{15}N = -4.5‰$), USGS 41 ($\delta^{15}N = 47.6‰$) and an in-house standard A + G ($\delta^{15}N = 5.4‰$). The $\delta^{15}N$ of the reagent blanks ranged from 1.6‰ to 3.1‰.

The oxidized samples were then transferred into new glass vials and readjusted to neutral pH by adding NaOH for the denitrifier method. The denitrifying bacterium Pseudomonas chlororaphis (strain ATCC 13985, Manassas, VA, USA), which lacks nitrous oxide reductase, was used to convert the nitrate in the sample into N_2O gas (Sigman et al., 2001). Typically, 1.5 mL of degassed bacterial concentrate was used for 5 nmol (of N) of sample injection. After sample injection, the culture was left overnight for complete conversion. The $\delta^{15}N$ of the N_2O was measured on a Thermo 253 plus isotope ratio mass spectrometer coupled with an N_2O extraction system. Two standard reference materials, IAEA-NO_3 (−1.8‰ vs. air) and USGS 34 (4.7‰ vs. air) were prepared every 8–10 samples to constrain the performance of the bacterial conversion and the stability of the mass spectrometer. The stability of the mass spectrometer was further monitored by a series of prepared N_2O gas vials at the beginning and the end of each run and every 10 samples. The N isotope composition is expressed as:

$$\delta^{15}N = \left(\frac{R_{\text{Sample}}}{R_{\text{Standard}}} - 1\right) \times 1000,$$

where R_{Sample} and R_{Standard} represent the $^{15}N/^{14}N$ ratios of sample and the air N_2, respectively. The average standard deviation of the $\delta^{15}N$ measurements was determined from an in-house coral standard measured repeatedly across runs, which showed about 0.2‰ standard deviation.

No replicate coral core was measured in this study due to resource constrain, however, previous studies of coral skeletal $\delta^{15}N$ reported small difference across colonies in oligotrophic open ocean (Ren et al., 2017; Wang et al., 2016), including one from SCS, where only 0.27‰ difference was observed between the two replicated cores across the 3-year-long overlapping periods (Ren et al., 2017).

2.4. Seawater Sampling, Nutrients, and Nitrate-$\delta^{15}N$ Measurement

Seawater sampling was conducted during a cruise onboard the R/V Shiyansanhao in September 2015 in the western SCS for proxy validation and identifying endmembers. Samples were collected from discrete depths (5, 25, 50, 75, 100, 150, 200, 300, 500, 800, 1000, and 1500 m) with a Seabird SBE 911 plus CTD (conductivity-temperature-density sensor) rosette system. Water for nutrient analysis was filtered through Millipore polycarbonate filters (0.2 μm) into acid-cleaned and sample-rinsed high-density polyethylene bottles (Nalgene) and stored at −20°C until analysis. Nitrate was determined as nitrate + nitrite by chemiluminescence after reduction to nitric oxide by an acidic solution of vanadium (V^{3+}) at 95°C, using a Teledyne 200 EU chemiluminescence analyzer. The concentration of phosphate was measured using a spectrophotometer via the standard molybdenum blue method (Hansen & Koroleff, 2007). The detection limit was 0.01 μM for nitrate and 0.02 μM for phosphate, respectively. The $\delta^{15}N$ of the seawater nitrate was determined using the denitrifier method for samples with [NO_3^-] greater than 0.3 μM. The average standard deviation of the $\delta^{15}N$ measurements on sample replicates was $<\pm 0.1‰$. Raw seawater nutrient data can be found in Figure S3 in Supporting Information S1.

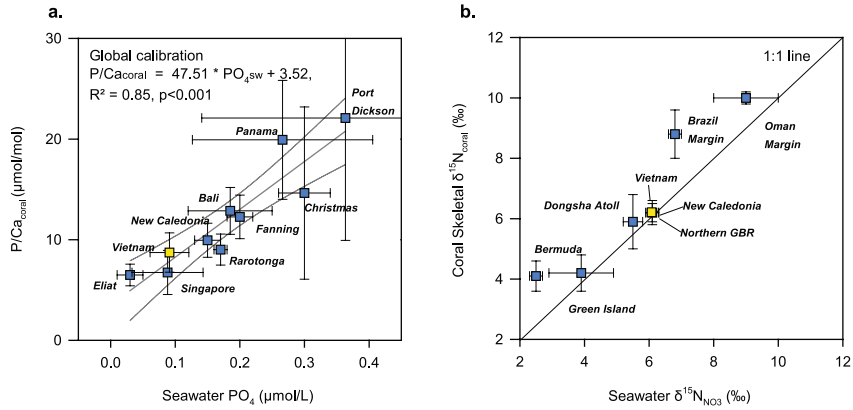

Figure 2. Calibration of coral skeletal P/Ca_{coral} (a) and $\delta^{15}N_{coral}$ (b) from the modern time Vietnam coral (yellow filled squares) with the global calibration. Other coral data were from M. Chen et al. (2019), (2022), and LaVigne et al. (2010) for P/Ca_{coral} and from Wang et al. (2016) for $\delta^{15}N_{coral}$.

3. Results and Discussion

3.1. Coral Proxy Validation

The modern part of (post 2000) coral P/Ca averaged at 8.73 ± 1.95 μmol/mol, and the measured seawater phosphate in the surface (top 20 mm) Western SCS was 0.09 ± 0.03 μmol/L (Figure S3 in Supporting Information S1). The Vietnam coral is this study is therefore consistent with the previously-reported calibration between P/Ca_{coral} and seawater phosphate across the globe (M. Chen et al., 2019; LaVigne et al., 2008) (Figure 2a), indicating that the P/Ca in our coral is representative of phosphate concentration in this region of the western SCS.

The $\delta^{15}N_{coral}$ values in the modern part of coral are 6.15‰ + 0.29‰, which compares well with the $\delta^{15}N$ in the subsurface nitrate 6.11‰ + 0.25‰ (Figure S3b in Supporting Information S1). This agreement is consistent with the previously identified relation between coral skeletal $\delta^{15}N_{coral}$ and subsurface nitrate (Wang et al., 2016) (Figure 2b), further supporting the case that in areas where surface nitrate is fully consumed, the coral $\delta^{15}N_{coral}$ is primarily a reflection of its N source.

In addition, bi-monthly sampling of the coral core for the years 1634, 1969, and 1994 is determined to assess the seasonal nutrient variabilities, which shows high P/Ca_{coral} and high $\delta^{15}N_{coral}$ values during the summer monsoon upwelling period, and low values during the other seasons (Figure S2 in Supporting Information S1), confirming that our coral tracks the expected monsoon-induced nutrient variability during both the LIA and modern times.

Our previous study identified a biological threshold of P/Ca_{coral} of ~6.3 μmol/mol, below which the P/Ca_{coral} is less or insensitive to seawater phosphate concentrations (M. Chen et al., 2019). Periods of low P/Ca_{coral} indeed appear in our record; specifically, out of the 134 samples analyzed covering the period of 1800–1960, 23 samples are below 6.3 μmol/mol, with an overall average of 7.8 ± 2.1 μmol/mol over 1800–1960. This period of low P/Ca_{coral} prevents a quantitative assessment of seawater phosphate using the record. Despite limitations for a quantitative assessment, the low P/Ca_{coral} strongly suggests that oligotrophic conditions prevailed during 1800–1960, as several studies using *Porites* coral living in oligotrophic environments across the world show similarly low P/Ca_{coral} (M. Chen et al., 2019, 2022; LaVigne et al., 2010). With part of the record approaching the biological threshold, extra caution is taken through sensitivity tests when we attempt to interpret coral P/Ca_{coral} record quantitatively in Section 3.3.

3.2. Enhanced Monsoon-Induced Upwelling During Little Ice Age

The down-core record of P/Ca_{coral} reveals large inter-annual variability in past phosphate concentrations. Within the coldest interval of the LIA (1600–1620, Figure 3), the P/Ca_{coral} averaged 22.63 μmol/mol. Subsequently, the P/Ca_{coral} decreased by a total of 65% in several successive steps: first to 16.00 μmol/mol in the 1630s, and then to 12.89 μmol/mol in the late 17th century. P/Ca_{coral} then decreased to below 10 μmol/mol from the 18th to the mid-20th century, until it started to increase slightly after the 1980s. After 2000, P/Ca_{coral} averaged at 8.73 μmol/mol.

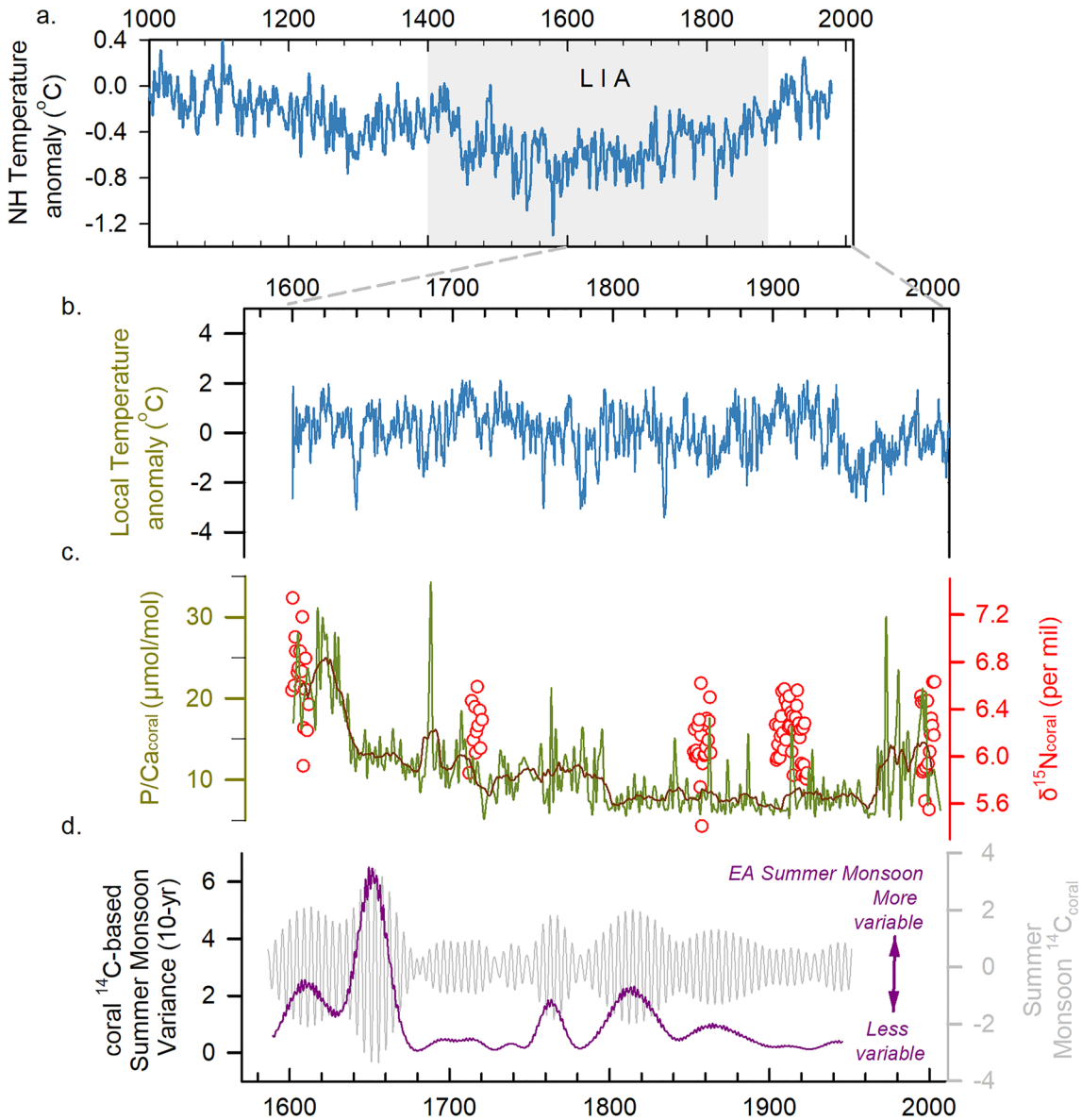

Figure 3. Comparison of Northern Hemisphere temperature anomaly versus coral proxy data. The time-series show (a) a multi-proxy reconstruction of Northern Hemisphere land and ocean surface temperature anomalies (blue lines) (Moberg et al., 2005); (b) annually resolved local sea surface temperature anomaly reconstructed from the same coral (Goodkin et al., 2021); (c) annually resolved coral skeletal phosphorus concentrations (P/Ca_{coral}, green) with a 10-year running average (brown); and coral skeletal nitrogen isotope composition ($\delta^{15}N_{coral}$, red open circles); and (d) annually resolved coral ^{14}C filtered at summer monsoon bands (gray) and its corresponding monsoonal wind variance (10-year-running variance, purple) (Goodkin et al., 2019). The period of the Little Ice Age (gray box) was defined according to (Mann, 2002).

Despite gaps in the $\delta^{15}N_{coral}$ record, a consistent decline in $\delta^{15}N_{coral}$ was also observed following the LIA: the $\delta^{15}N_{coral}$ averaged 6.68‰ ± 0.35‰ during 1600–1610, which is significantly higher than all the later periods analyzed (average 6.15‰ ± 0.29‰ for 1710–1720, 1850–1860, 1900–1920, and 1991–2000, $\Delta\delta^{15}N_{coral} = +0.53‰$, $p < 0.0001$, ANOVA, Figure 3; Table S1 in Supporting Information S1). Hydrographic stations in the SCS show that the average $\delta^{15}N_{NO3}$ in subsurface waters (400 m) is ~6‰ (Figure 1; Figure S3 in Supporting Information S1). This value is much higher than the $\delta^{15}N_{NO3}$ generated by nitrogen fixation (−1‰) (Montoya et al., 2002), which is the other main source of N to the surface ocean here. Therefore, changes in the $\delta^{15}N_{coral}$ record indicate significant changes in the relative contributions of N fixation and subsurface nitrate from the LIA to the present.

The combined results of both proxies therefore indicate large, low-frequency changes in nutrient supply to the surface SCS. Crucially, the concurrent changes in P/Ca_{coral} and $\delta^{15}N_{coral}$ show that this biogeochemical variability

involved mechanisms that increased the concurrent supply of N and P to the surface ocean, instead of just changes in N fixation or changes to the isotopic composition of the subsurface nitrate pool that only alters the $\delta^{15}N_{coral}$. These changes preceded the major warming in the Northern Hemisphere at the end of LIA by at least 150 years, and no warming trend is found at this site during this time (Figure 3) (Goodkin et al., 2021), suggesting that these changes are unlikely to result from increased stratification through warming. The changes also precede anthropogenic impacts such as fertilizer influx (Marion et al., 2005) or atmospheric deposition (Ren et al., 2017), which only occurred in the late 20th century. For the observed biogeochemical conditions to have been met during the LIA, changes to riverine nutrient input and/or subsurface nutrient upwelling would have had to occur.

Greater riverine inputs of nutrients during the LIA are unlikely to account for the variation in our coral record. Hydrological reconstructions from a carbonate lake sediment in northern Vietnam (Stevens et al., 2018) and multiple tree ring records across Vietnam (Buckley et al., 2017) clearly show drier regional climate during the 17th century (Figure S4 in Supporting Information S1). Therefore, the most likely explanation for the higher P/Ca_{coral} and $\delta^{15}N_{coral}$ observed during the LIA is enhanced monsoon-induced upwelling of nutrient-rich subsurface water. The southwest monsoon winds initiate and maintain seasonal upwelling in the western SCS (Xie et al., 2003). The southwest monsoon wind strength is also predicted by a cohort of General Circulation Models (GCMs) to be strongly tied to surface ocean upward velocity (Figure S5 in Supporting Information S1). Our nutrient proxy data, therefore, imply an overall stronger southwest monsoon wind at our site during the peak of the LIA.

We compared our P/Ca_{coral} and $\delta^{15}N_{coral}$ data to a record of summer monsoon variance generated from the same coral using $\Delta^{14}C$ as a proxy for summer wind-driven upwelling. During the LIA, higher P/Ca_{coral} and $\delta^{15}N_{coral}$ coincide with periods of increased ^{14}C-based summer monsoon variance (Figure 3) (Goodkin et al., 2019). While the $\Delta^{14}C$ indicates more variable summer monsoon winds during this period, the nutrient data extends the interpretation to a more variable and stronger summer monsoon during the LIA.

The P/Ca in the modern part of the coral (1851–1955, post 1955 was not assessed due to uncertain contribution of anthropogenic P) does not correlate with the record of summer monsoon wind stress, possibly because the seawater phosphate concentration was too low, in which the P/Ca in coral reached a biological threshold that estimated in the literature to be less/not sensitive to the seawater variabilities (Figure S6 in Supporting Information S1). Despite the lack of correlation with summer monsoon wind over the modern period, spectral analysis of P/Ca indicates significant power at 2–3 year periods (95% confidence level) (Figure S7 in Supporting Information S1), in agreement with the power found in East Asian Summer Monsoon records (F. Chen et al., 2013; Shen & Lau, 1995; W. Wang et al., 2014). To further constrain the magnitude of the changes in nutrient supply we developed two box models.

3.3. The Extent of Biogeochemical Response

With the $\delta^{15}N_{coral}$ record, the decadal average $\delta^{15}N_{coral}$ allows us to build a 1-D box model (Text S1 in Supporting Information S1) to estimate the fractional changes in N supply to the coral site over periods of data coverage, which corresponds to peak LIA time and four windows in modern times. N from fixation has a $\delta^{15}N$ value of −1.0‰ (Montoya et al., 2002), and the upward supply of subsurface nitrate has a $\delta^{15}N$ value of 6.0‰, based on in-situ measurements (Figure 4a). We assume that the present-day downward export of particulate N has a $\delta^{15}N$ value equal to the $\delta^{15}N_{NO3}$ measured immediately below the euphotic zone, which averages ∼4.45‰ in the western SCS (Figure S3 in Supporting Information S1). Based on these end members, our box model suggests that in the present day, ∼22% of the surface ocean nitrate pool in the western SCS is derived from N fixation and ∼78% from subsurface nitrate supply. If the N fixation rate during the LIA was equal to our estimated present-day rate, our model shows that the subsurface nitrate supply must have been ∼48% greater than today's total N supply to account for the 0.53‰ increase in $\delta^{15}N_{coral}$ (Figure 3b; constant N fixation scenario, Text S1 in Supporting Information S1). This scenario serves as an upper-bound estimate of the increased upwelling of subsurface nutrients during the LIA. Because an increase in nitrate supply to surface waters would relax N limitation, it is more likely that N fixation would have been lower during the LIA (Loick et al., 2007). Therefore, we ran a second model simulation, assuming that the increase in subsurface nitrate supply caused a decrease in N fixation by the same amount, so that the total N supply to the surface ocean was the same during the LIA as during the present (constant total flux scenario, Text S1 in Supporting Information S1). This scenario serves as a lower-bound estimate of the change in subsurface nutrient supply and indicates that the upwelling of subsurface nitrate during

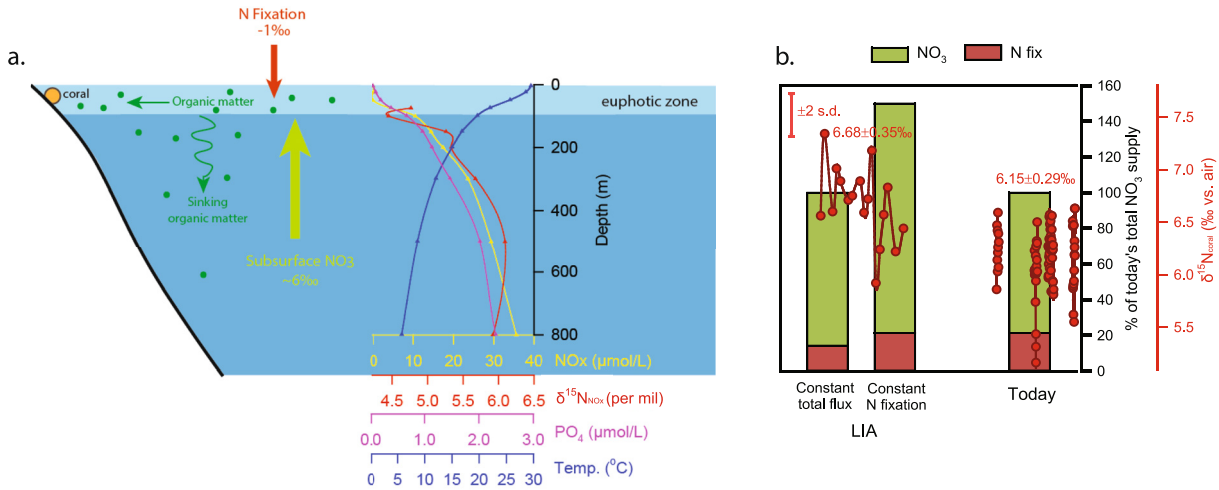

Figure 4. Model of nutrient cycling in the South China Sea. (a) The main sources of nitrogen to our coral are nitrogen fixation (red arrow, $\delta^{15}N = -1‰$) and upwelling of subsurface nitrate (yellow arrow, $\delta^{15}N = 6‰$). The depth profiles of temperature, $\delta^{15}N_{NO3}$, nitrate, and phosphate are also shown. (b) A box model calculation shows that to achieve the 0.53‰ increase in $\delta^{15}N_{coral}$ during the Little Ice Age (17th century), the net subsurface nitrate supply would have had to be at least 8% greater with reduced nitrogen fixation (constant total flux scenario); or up to 48% higher with nitrogen fixation remaining unchanged (constant N fixation scenario). The percentages were all calculated relative to the present-day total N supply.

the LIA was at least ~8% greater than today's total N supply. However, this scenario also shows that N fixation must have been 52% higher than at present, which would likely entail a major phytoplankton community shift (Figure 4b; constant total flux scenario, Text S1 in Supporting Information S1). Our isotope box model, therefore, suggests that the western SCS may have undergone substantial oligotrophication since the 17th Century, resulting in an increase in N fixation and possibly a significant phytoplankton community shift (Table S2 in Supporting Information S1).

Analysis of the temporally complete P/Ca_{coral} record supports these findings. The average P/Ca_{coral} for the present (1800–1970 combined) and peak LIA (1600–1620) is 7.95 μmol/mol, and 22.63 μmol/mol, which indicates significant decrease in seawater phosphate concentration, respectively. The retention of seawater phosphate within surface ocean could be assessed using residence time calculations. The residence time of phosphate in the surface ocean can be calculated as:

$$\tau_{p-\text{today}} = \frac{\text{DIP}_{\text{today}} * \text{MLD}}{f_{p-\text{today}}} \quad (1)$$

$$\tau_{p-\text{LIA}} = \frac{\text{DIP}_{\text{LIA}} * \text{MLD}}{\text{f}_{\text{p-LIA}}} \quad (2)$$

where the $\tau_{p-\text{today}}$ and $\tau_{p-\text{LIA}}$ are the residence time of P in the surface ocean, the $f_{p-\text{today}}$ and $f_{p-\text{LIA}}$ are the unit area rates of P supply within the mixed layer, the $\text{DIP}_{\text{today}}$ and DIP_{LIA} are the surface ocean dissolved inorganic phosphate, and the MLD is the mix layer depth. Assuming relative changes in subsurface nutrient supply predicted by N isotope model, we can subsequently calculate that the residence time of P in the surface ocean over LIA was 2.68–3.93 times of today (see detailed calculation in Text S2 in Supporting Information S1), suggesting accumulation of P within the surface ocean during LIA times. Our calculation makes the simplifying assumption that the mixed layer depth was the same in the LIA as nowadays. Because in a tropical ocean, higher subsurface nutrient flux from stronger upwelling would result in a shallower mixed layer, our calculation is likely an upper boundary of the increased residence time of P in the mixed layer. Besides the assumption of constant mixed layer depth, our calculation also makes a simplifying assumption by using the slope of global P/Ca_{coral}-phosphate calibration (Figure 2a) since a local calibration is unavailable. However, such calibrations have shown variability across colonies (LaVigne et al., 2010). The potential impact on the residence time of P by the uncertainty in calibration was assessed through a sensitivity test, in which we varied the slope of P/Ca_{coral}-phosphate calibration over ±40%, which bracketed all the observed variabilities in P/Ca_{coral}-phosphate calibrations across the world (±36%, $n = 5$ colonies) (M. Chen et al., 2019, 2022; LaVigne et al., 2010). The variation in P/Ca_{coral}-phosphate calibration

results in the calculated residence time over the LIA ranging from 2.14 to 6.12 times greater than today (see detailed calculation in Text S2 in Supporting Information S1), indicating more than 50% decline in P residence time from LIA to today. Clearly, even the lower bound of this range still supports our conclusion of P accumulation during the LIA despite the uncertainties in proxy calibration. Overall, the nearly 65% decrease in P/Ca_{coral} during the 17th Century is qualitatively consistent with major climate-driven oligotrophication as illustrated in the N isotope box model and implies a major decrease in the residence time of P in the surface western SCS after the peak of the LIA (Text S2 in Supporting Information S1).

Monsoon-driven upwelling occurs in other areas around the SCS, such as islands off southern China. Paleo-records of guano deposits and bone collagen $\delta^{15}N$ in the Xisha Islands (~600 km northeast of our site) show that seabird populations declined drastically (Xu et al., 2016), and experienced dietary changes following the LIA peak (Wu et al., 2016). Since seabird populations are generally thought to be strongly controlled by food availability (Cury et al., 2011), the changes in the seabird population at the Xisha Islands concurrent with our coral records indicate that changes in monsoonal winds and surface nutrients probably occurred across a wider geographical area at that time.

3.4. Implications for Future Climate Change

Continued anthropogenic climate change is predicted to strengthen thermal stratification throughout the oceans and reduce net primary productivity by trapping nutrients at depth (Fu et al., 2016; Moore et al., 2018; Pachauri et al., 2014). Deep-sea coral-based reconstructions of N fixation (Sherwood et al., 2014) and plankton community composition (McMahon et al., 2015) since the LIA in the North Pacific Subtropical Gyre suggest that recently observed decadal variations in surface biogeochemistry are part of a centennial-scale oligotrophication trend and that N fixation has partly balanced the reduction of nutrient supply. Although global ocean biogeochemical models predict that net primary production in tropical regions will decrease as a result of climate change, large differences between projections are seen at regional scales (Boyd et al., 2014). Our coral record shows oligotrophication in the SCS since the LIA, but also indicates that the nutrient dynamics of the SCS are tightly linked to the strength of the East Asian Summer Monsoon winds. With ongoing anthropogenic climate change, the East Asian Summer Monsoon is generally expected to intensify and become more variable (Liu et al., 2020; Pachauri et al., 2014; Sun & Ding, 2010), potentially returning nutrient conditions to those seen during the initial onset of the LIA. The implication of our results is therefore that climate change-driven intensification of summer monsoon upwelling may lead to increases in nutrient supply to the SCS. The East Asian Monsoon is one of the world's largest monsoon systems and has a profound influence on the biogeochemistry of many marginal seas and coastal regions in addition to the SCS (P. Wang et al., 2019). Given the large human population density surrounding these marginal seas, and the heavy dependence of these societies on marine food resources (Costello et al., 2020), accurate predictions of ocean biogeochemical responses to the changing climate are urgently needed. Increased observations of past variability in biogeochemical cycling during well-characterized periods of climate change are necessary to understand these important biogeochemical controls and help predict how they will change in the future.

Conflict of Interest

The authors declare no conflicts of interest relevant to this study.

Data Availability Statement

Data associated with this study can be found at the Supporting Information S1 or at M. Chen et al. (2023).

Acknowledgments
Thanks go to G. Williams, W. Tak-Cheung, and J. Ossolinski for field assistance; the World Climate Research Programme which, through its climate modeling groups for making available their model output; the Earth System Grid Federation (ESGF) for archiving the data and providing access; and the multiple funding agencies who support CMIP6 and ESGF. We thank Mr. Liu Jinjingyuan for performing statistical tests; Ms. Su Ping Heng and Ms. Dora Hui Xuan Tay for laboratory assistance.
The research was supported by the Singapore Ministry of Education Academic Research Fund Tier 2 (award MOE2016-T2-1-016 to N. F. G. and K. A. H.), by the Earth Observatory of Singapore and the Singapore Ministry of Education under the Research Centers of Excellence initiative, and by the Taiwan Ministry of Science and Technology (MOST 110-2636-M-002-002- to H. R.)

References

Bolton, A., Goodkin, N. F., Hughen, K., Ostermann, D. R., Vo, S. T., & Phan, H. K. (2014). Paired Porites coral Sr/Ca and δ18O from the western South China Sea: Proxy calibration of sea surface temperature and precipitation. *Palaeogeography, Palaeoclimatology, Palaeoecology*, *410*, 233–243. https://doi.org/10.1016/j.palaeo.2014.05.047

Boyd, P. W., Sundby, S., & Pörtner, H.-O. (2014). Cross-chapter box on net primary production in the ocean. In *Climate change 2014: Impacts, adaptation, and vulnerability. Part A: Global and sectoral aspects. Contribution of Working Group II to the fifth assessment report of the intergovernmental panel of climate change* (pp. 133–136). Cambridge University Press.

Buckley, B. M., Palakit, K., Duangsathaporn, K., Sanguantham, P., & Prasomsin, P. (2007). Decadal scale droughts over northwestern Thailand over the past 448 years: Links to the tropical Pacific and Indian Ocean sectors. *Climate Dynamics*, *29*(1), 63–71. https://doi.org/10.1007/s00382-007-0225-1

Buckley, B. M., Stahle, D. K., Luu, H. T., Wang, S.-Y. S., Nguyen, T. Q. T., Thomas, P., et al. (2017). Central Vietnam climate over the past five centuries from cypress tree rings. *Climate Dynamics*, *48*(11), 3707–3723. https://doi.org/10.1007/s00382-016-3297-y

Chen, F., Yuan, Y.-J., Wei, W.-S., Fan, Z.-A., Yu, S.-l., Zhang, T.-W., et al. (2013). Reconstructed precipitation for the north-central China over the past 380 years and its linkages to East Asian summer monsoon variability. *Quaternary International*, *283*, 36–45. https://doi.org/10.1016/j.quaint.2012.05.047

Chen, M., Chia, H. K., Martin, P., Lee, J. N., Bettens, R. P. A., & Tanzil, J. T. I. (2022). A half-century record of coral skeletal P/Ca reveals late 20th century nutrient pollution in Port Dickson, Malaysia. *Marine Pollution Bulletin*, *181*, 113875. https://doi.org/10.1016/j.marpolbul.2022.113875

Chen, M., Martin, P., Goodkin, N. F., Tanzil, J., Murty, S., & Wiguna, A. A. (2019). An assessment of P speciation and P: Ca proxy calibration in coral cores from Singapore and Bali. *Geochimica et Cosmochimica Acta*, *267*, 113–123. https://doi.org/10.1016/j.gca.2019.09.024

Chen, M., Martin, P., Ren, H., Zhang, R., Samanta, D., Chen, Y.-C., et al. (2023). Data for Enhanced monsoon-driven upwelling in Southeast Asia during the Little Ice Age [Dataset]. ScholarBank@NUS Repository. https://doi.org/10.25540/TJ9G-S18F

Costello, C., Cao, L., Gelcich, S., Cisneros-Mata, M. Á., Free, C. M., Froehlich, H. E., et al. (2020). The future of food from the sea. *Nature*, *588*(7836), 95–100. https://doi.org/10.1038/s41586-020-2616-y

Cury, P. M., Boyd, I. L., Bonhommeau, S., Anker-Nilssen, T., Crawford, R. J. M., Furness, R. W., et al. (2011). Global Seabird response to forage fish depletion—One-third for the birds. *Science*, *334*(6063), 1703–1706. https://doi.org/10.1126/science.1212928

Dodge, R. E., Jickells, T. D., Knap, A. H., Boyd, S., & Bak, R. P. M. (1984). Reef-building coral skeletons as chemical pollution (phosphorus) indicators. *Marine Pollution Bulletin*, *15*(5), 178–187. https://doi.org/10.1016/0025-326X(84)90317-5

Doherty, J. M., Williams, B., Kline, E., Adey, W., & Thibodeau, B. (2021). Climate-modulated nutrient conditions along the Labrador Shelf: Evidence from nitrogen isotopes in a six-hundred-year-old crustose coralline alga. *Paleoceanography and Paleoclimatology*, *36*(5), e2020PA004149. https://doi.org/10.1029/2020pa004149

Fu, W., Randerson, J. T., & Moore, J. K. (2016). Climate change impacts on net primary production (NPP) and export production (EP) regulated by increasing stratification and phytoplankton community structure in the CMIP5 models. *Biogeosciences*, *13*(18), 5151–5170. https://doi.org/10.5194/bg-13-5151-2016

Garcia, H. E., Locarnini, R. A., Boyer, T. P., Antonov, J. I., Baranova, O. K., Zweng, M. M., et al. (2013). World ocean atlas 2013. Dissolved inorganic nutrients (phosphate, nitrate, silicate) (Vol. *4*).

Goodkin, N. F., Bolton, A., Hughen, K., Karnauskas, K., Griffin, S., Phan, K., et al. (2019). East Asian Monsoon variability since the sixteenth century. *Geophysical Research Letters*, *46*(9), 4790–4798. https://doi.org/10.1029/2019gl081939

Goodkin, N. F., Samanta, D., Bolton, A., Ong, M. R., Hoang, P. K., Vo, S. T., et al. (2021). Natural and anthropogenic forcing of multi-decadal to centennial scale variability of sea surface temperature in the South China Sea. *Paleoceanography and Paleoclimatology*, *36*(10), e2021PA004233. https://doi.org/10.1029/2021PA004233

Grosse, J., Bombar, D., Doan, H. N., Nguyen, L. N., & Voss, M. (2010). The Mekong River plume fuels nitrogen fixation and determines phytoplankton species distribution in the South China Sea during low and high discharge season. *Limnology and Oceanography*, *55*(4), 1668–1680. https://doi.org/10.4319/lo.2010.55.4.1668

Hansen, H. P., & Koroleff, F. (2007). Determination of nutrients. In K. Grasshoff, K. Kremling, & M. Ehrhardt (Eds.), *Methods of seawater analysis*. https://doi.org/10.1002/9783527613984.ch10

Jiang, W., Yang, H., Yu, K., Song, Y., Zhao, J. X., Feng, Y. X., et al. (2020). Porites coral on a remote reef reveal marine phosphorus biogeochemical cycling following artificial disturbance. *Journal of Geophysical Research: Oceans*, *125*(8), e2020JC016388. https://doi.org/10.1029/2020jc016388

LaVigne, M., Field, M. P., Anagnostou, E., Grottoli, A. G., Wellington, G. M., & Sherrell, R. M. (2008). Skeletal P/Ca tracks upwelling in Gulf of Panamá coral: Evidence for a new seawater phosphate proxy. *Geophysical Research Letters*, *35*(L05604), L05604. https://doi.org/10.1029/2007GL031926

LaVigne, M., Matthews, K. A., Grottoli, A. G., Cobb, K. M., Anagnostou, E., Cabioch, G., & Sherrell, R. M. (2010). Coral skeleton P/Ca proxy for seawater phosphate: Multi-colony calibration with a contemporaneous seawater phosphate record. *Geochimica et Cosmochimica Acta*, *74*(4), 1282–1293. https://doi.org/10.1016/j.gca.2009.11.002

Liu, Y., Li, Y., & Ding, Y. (2020). East Asian summer rainfall projection and uncertainty under a global warming scenario. *International Journal of Climatology*, *40*(11), 4828–4842. https://doi.org/10.1002/joc.6491

Loick, N., Dippner, J., Doan, H. N., Liskow, I., & Voss, M. (2007). Pelagic nitrogen dynamics in the Vietnamese upwelling area according to stable nitrogen and carbon isotope data. *Deep Sea Research Part I: Oceanographic Research Papers*, *54*(4), 596–607. https://doi.org/10.1016/j.dsr.2006.12.009

Loick-Wilde, N., Bombar, D., Doan, H. N., Nguyen, L. N., Nguyen-Thi, A. M., Voss, M., & Dippner, J. W. (2017). Microplankton biomass and diversity in the Vietnamese upwelling area during SW monsoon under normal conditions and after an ENSO event. *Progress in Oceanography*, *153*, 1–15. https://doi.org/10.1016/j.pocean.2017.04.007

Mallela, J., Lewis, S. E., & Croke, B. (2013). Coral skeletons provide historical evidence of phosphorus runoff on the great barrier reef. *PLoS One*, *8*(9), e75663. https://doi.org/10.1371/journal.pone.0075663

Mann, M. E. (2002). Little ice age. *Encyclopedia of global environmental change*, *1*(504), e509.

Marion, G. S., Dunbar, R. B., Mucciarone, D. A., Kremer, J. N., Lansing, J. S., & Arthawiguna, A. (2005). Coral skeletal δ15N reveals isotopic traces of an agricultural revolution. *Marine Pollution Bulletin*, *50*(9), 931–944. https://doi.org/10.1016/j.marpolbul.2005.04.001

McMahon, K. W., McCarthy, M. D., Sherwood, O. A., Larsen, T., & Guilderson, T. P. (2015). Millennial-scale plankton regime shifts in the subtropical North Pacific Ocean. *Science*, *350*(6267), 1530–1533. https://doi.org/10.1126/science.aaa9942

Moberg, A., Sonechkin, D. M., Holmgren, K., Datsenko, N. M., & Karlén, W. (2005). Highly variable Northern Hemisphere temperatures reconstructed from low-and high-resolution proxy data. *Nature*, *433*(7026), 613–617. https://doi.org/10.1038/nature03265

Montoya, J. P., Carpenter, E. J., & Capone, D. G. (2002). Nitrogen fixation and nitrogen isotope abundances in zooplankton of the oligotrophic North Atlantic. *Limnology and Oceanography*, *47*(6), 1617–1628. https://doi.org/10.4319/lo.2002.47.6.1617

Moore, J. K., Fu, W., Primeau, F., Britten, G. L., Lindsay, K., Long, M., et al. (2018). Sustained climate warming drives declining marine biological productivity. *Science*, *359*(6380), 1139–1143. https://doi.org/10.1126/science.aao6379

Nguyen, T. A., Phan, M. T., Nguyen, H. H., & Ittekkot, V. (2000). Tracing sediment transport and bed regime in Nha Trang Bay.

Pachauri, R. K., Allen, M. R., Barros, V. R., Broome, J., Cramer, W., Christ, R., et al. (2014). *Climate change 2014: Synthesis report. Contribution of Working Groups I, II and III to the fifth assessment report of the Intergovernmental Panel on Climate Change*. IPCC.

Ren, H., Chen, Y.-C., Wang, X. T., Wong, G. T. F., Cohen, A. L., DeCarlo, T. M., et al. (2017). 21st-century rise in anthropogenic nitrogen deposition on a remote coral reef. *Science*, *356*(6339), 749–752. https://doi.org/10.1126/science.aal3869

Sale, P. F., Agardy, T., Ainsworth, C. H., Feist, B. E., Bell, J. D., Christie, P., et al. (2014). Transforming management of tropical coastal seas to cope with challenges of the 21st century. *Marine Pollution Bulletin*, *85*(1), 8–23. https://doi.org/10.1016/j.marpolbul.2014.06.005

Sallée, J. B., Shuckburgh, E., Bruneau, N., Meijers, A. J., Bracegirdle, T. J., & Wang, Z. (2013). Assessment of Southern Ocean mixed-layer depths in CMIP5 models: Historical bias and forcing response. *Journal of Geophysical Research: Oceans*, *118*(4), 1845–1862. https://doi.org/10.1002/jgrc.20157

Shen, S., & Lau, K. M. (1995). Biennial oscillation associated with the East Asian summer monsoon and tropical sea surface temperatures. *Journal of the Meteorological Society of Japan: Series II*, *73*(1), 105–124. https://doi.org/10.2151/jmsj1965.73.1_105

Sherwood, O. A., Guilderson, T. P., Batista, F. C., Schiff, J. T., & McCarthy, M. D. (2014). Increasing subtropical North Pacific Ocean nitrogen fixation since the Little Ice Age. *Nature*, *505*(7481), 78–81. https://doi.org/10.1038/nature12784

Sigman, D. M., Casciotti, K. L., Andreani, M., Barford, C., Galanter, M., & Böhlke, J. (2001). A bacterial method for the nitrogen isotopic analysis of nitrate in seawater and freshwater. *Analytical Chemistry*, *73*(17), 4145–4153. https://doi.org/10.1021/ac010088e

Stevens, L. R., Buckley, B. M., Kim, S., Hill, P., & Doiron, K. (2018). Increased effective moisture in northern Vietnam during the Little Ice Age. *Palaeogeography, Palaeoclimatology, Palaeoecology*, *511*, 449–461. https://doi.org/10.1016/j.palaeo.2018.09.011

Stobutzki, I. C., Silvestre, G. T., Talib, A. A., Krongprom, A., Supongpan, M., Khemakorn, P., et al. (2006). Decline of demersal coastal fisheries resources in three developing Asian countries. *Fisheries Research*, *78*(2–3), 130–142. https://doi.org/10.1016/j.fishres.2006.02.004

Sun, Y., & Ding, Y. H. (2010). A projection of future changes in summer precipitation and monsoon in East Asia. *Science China Earth Sciences*, *53*(2), 284–300. https://doi.org/10.1007/s11430-009-0123-y

Wang, P., Clemens, S. C., Tada, R., & Murray, R. W. (2019). Blowing in the monsoon wind. *Oceanography*, *32*(1), 48–59. https://doi.org/10.5670/oceanog.2019.119

Wang, W., Zhou, W., & Chen, D. (2014). Summer high temperature extremes in southeast China: Bonding with the El Niño–Southern Oscillation and East Asian summer monsoon coupled system. *Journal of Climate*, *27*(11), 4122–4138. https://doi.org/10.1175/jcli-d-13-00545.1

Wang, X. T., Sigman, D. M., Cohen, A., Sinclair, D., Sherrell, R., Weigand, M., et al. (2015). Isotopic composition of skeleton-bound organic nitrogen in reef-building symbiotic corals: A new method and proxy evaluation at Bermuda. *Geochimica et Cosmochimica Acta*, *148*, 179–190. https://doi.org/10.1016/j.gca.2014.09.017

Wang, X. T., Sigman, D. M., Cohen, A. L., Sinclair, D. J., Sherrell, R. M., Cobb, K. M., et al. (2016). Influence of open ocean nitrogen supply on the skeletal δ15N of modern shallow-water scleractinian corals. *Earth and Planetary Science Letters*, *441*, 125–132. https://doi.org/10.1016/j.epsl.2016.02.032

Wu, L., Liu, X., Fu, P., Xu, L., Li, D., & Li, Y. (2016). Dietary change in seabirds on Guangjin Island, South China Sea, over the past 1200 years inferred from stable isotope analysis. *The Holocene*, *27*(3), 331–338. https://doi.org/10.1177/0959683616660163

Xie, S.-P., Xie, Q., Wang, D., & Liu, W. T. (2003). Summer upwelling in the South China Sea and its role in regional climate variations. *Journal of Geophysical Research*, *108*(C8), 3261. https://doi.org/10.1029/2003jc001867

Xu, L., Liu, X., Wu, L., Sun, L., Zhao, J., & Chen, L. (2016). Decline of recent seabirds inferred from a composite 1000-year record of population dynamics. *Scientific Reports*, *6*(1), 35191. https://doi.org/10.1038/srep35191

Zheng, J., Xiao, L., Fang, X., Hao, Z., Ge, Q., & Li, B. (2014). How climate change impacted the collapse of the Ming dynasty. *Climatic Change*, *127*(2), 169–182. https://doi.org/10.1007/s10584-014-1244-7